

# Coloring Effect of the Organic Hybrid of Polyamide 6 and *N,N'*-ethylene-bis(tetrabromophthalimide)

Xin Deng, Wen-Li Dai, Yun-Long Zheng

Department of Polymer Science and Engineering, Chemistry College, Xiangtan University, Xiangtan 411105, People's Republic of China

Received 6 January 2006; accepted 10 March 2006

DOI 10.1002/app.25613

Published online in Wiley InterScience (www.interscience.wiley.com).

**ABSTRACT:** Coloring study in organic hybrid of polyamide (PA6) and *N,N'*-ethylene-bis(tetrabromophthalimide) (EPT), where the chromophore was self-assembled by hydrogen bonding formed between PA6 molecular chains and EPT compound, have been characterized by several techniques. CS930 double wavelength lamella scanner was employed to measure the change of color. The existence of hydrogen bonding in PA6/*N,N'*-ethylene-bis(tetrabromophthalimide) (PA6EPT) was investigated with Fourier transform infrared (FTIR), the results of which were compared with that of PA6 with the same thermal history. FTIR spectra at room temperature revealed that there is essentially hydrogen bonding between PA6 and EPT. The crystallization behavior of PA6EPT affected by hydrogen bonding was studied by using FTIR. The temperature-dependent behavior of both PA6 and PA6EPT

was studied by temperature-FTIR spectroscopy and differential scanning calorimetry (DSC). With temperature increasing, changes in sensitive, high-resolution absorbance spectra are observed as dissolve-volatilizing thin film. Temperature-FTIR results showed that the hydrogen bonding in PA6EPT attenuated and dissociated considerably at a smaller rate than PA6, that is to say, hydrogen bonding in PA6EPT is more stable than that in PA6. DSC showed that the melting temperature of PA6EPT and PA6 are similar. However, the crystalline degree and crystalline temperature and melting enthalpy of PA6 and PA6EPT are different. © 2007 Wiley Periodicals, Inc. *J Appl Polym Sci* 104: 594–600, 2007

**Key words:** hydrogen bonding; polyamide 6; EPT; color; FTIR

## INTRODUCTION

It is well-known that there are some methods in coloring technology of polymer<sup>1</sup>: (1) Coloration with single pigment. Many types of colorants (dyes, organic or inorganic pigments, and some specialty compounds) were used directly in the coloring process of resins or plastics. In the coloring technology, colors can be matched according to optical principles for the color that we need. The colorants are dry blended with the plastic granules at room temperature in a mixer. But the properties of materials would be affected when the colorants are added into plastics or resins; if inadequate dispersion of a pigment appears in polymer systems, it would manifest many limitations, such as fluctuations in color intensity, deviations in shade, and drop in mechanical strength. (2) Coloration with pigment concentrates. This processing technique is the same as that described when using single pigments, but possesses the advantages that the pigments are already present in an optimally dispersed form. In the methods

above-mentioned, proper colorants need to be selected to make polymer appear the color of colorants. But in the engineering polymer, there are some problems in the compatibility between polymer and colorants: (1) thermal stability, lightfastness, and weather resistance of colored polymer; (2) the property of migration. Because of long contact between colored products and solid, solvent, or gas, chemical or physical reaction will take place. Then, pigment particle will migrate from the plastics/pigment system to the surface, or the colorants will migrate to nearby objects. Since the addition of an adhesion promoter or a dispersing agent can influence the properties of materials, the compatibility between polymer and colorants is very important problem. It is well-known that chromophore in the pigment structure is an important reason for coloring polymers. Many researchers have taken some experiments to resolve the above-mentioned problems, such as chromophores can be introduced into polymer's main chain<sup>2–4</sup> or bonded as a side group<sup>5,6</sup> and can be dissolved in a polymer matrix.<sup>7–9</sup> In this study, noncovalent interactions are being used in preparation of chromophore. We recently have found that intermolecular hydrogen bonding, which will come into being between *N,N'*-ethylene-bis(tetrabromophthalimide) (EPT) with a polar functional group and PA6 macromolecular material with a polar atom, can self-assemble into chromophore, and then the PA6

Correspondence to: W.-L. Dai (daiwenlip@163.com).

Contract grant sponsor: Hunnan Provincial Educational Department; contract grant number: 02C576.

material is colored. It is a new domain in the coloring technology.

In this study, Fourier transform infrared (FTIR), temperature-FTIR, and DSC were used to identify the existence and effect on crystallization behavior of hydrogen bonding and temperature-dependent behavior of hydrogen bonding, respectively. On the basis of these experimental evidences, these studies attempted to describe the thermal stability of hydrogen bonding and interpret the crystallization property of colored PA6 obtained by hydrogen bonding.

## EXPERIMENTAL

### Materials

PA6 was purchased from Baling Company, China Petroleum and Chemical, relative viscosity ( $\eta_r$ ) = 3.33; The EPT was prepared by bromination of *N-N'*-ethylene-bis(phthalimide) (EBP), which was synthesized with *o*-phthalic anhydride and 1,2-diaminocethane as reactants and water as reaction media.<sup>10</sup>

In the experiments, the different ratios of PA6/EPT have been taken; the color belongs to the same series. So, the 95/5 (by weight) ratio of PA6/EPT was studied for achieving saturated hydrogen bonding between PA6 molecular chains and EPT and taking visible experimental effect. It was prepared using a twin-screw extruder (SHJ-30A, Nanjing Plastics Machinery Plant, China), which was operated at a screw revolution of 100 rpm and a temperature profile of 225–240°C.

### Measurement

#### Visible chromatogram

CS930 double wavelength lamella scanner (JN) was employed to measure reflect spectrum of PA6, EPT, and PA6EPT for analyzing change of the color. The testing samples: EPT sample is powder; both PA6 and PA6EPT are strip samples, the dimension ( $l \times w \times h$ ): 120 × 10 × 4 mm<sup>3</sup>.

#### Fourier transform infrared spectroscopy

Infrared spectra were taken with a Spectrum One B FTIR spectrometer (PE Comp. American), and the FTIR spectra at different temperature were obtained by using FTIR spectrometer equipped with a variable-temperature cell. To obtain a thin smooth film for IR study, the particle samples were dissolved in formic acid, and thin film samples were obtained by flow of liquor in the glass plate because solvent is volatile at room temperature. The films were dried in a vacuum oven, at 100°C for 8 h, before use. The thin films were scanned at room temperature to prove the existence of hydrogen bonding. And the samples were scanned in the wavenumber range

from 4000 to 450 cm<sup>-1</sup>. The spectra at different temperature are acquired by temperature-FTIR. The samples were scanned at an increasing interval of 20°C until the temperature nears melting point of PA6 (230°C); the specific temperatures are: 30, 50, 70, 90, 110, 130, 150, 170, 190, 210, and 230°C. Before spectra collection, the cell was equilibrated for at least 2 min at each temperature.

#### Differential scanning calorimetry

The crystallization experiments were performed in a TA Instruments Q10 modulated differential scanning calorimeter (DSC) with a sample weight of 5–8 mg under a nitrogen atmosphere. The samples were encapsulated into aluminum pans and were heated to 250°C at 10°C/min rate, and the heat flow during crystallization was recorded as a function of temperature.

## RESULTS AND DISCUSSION

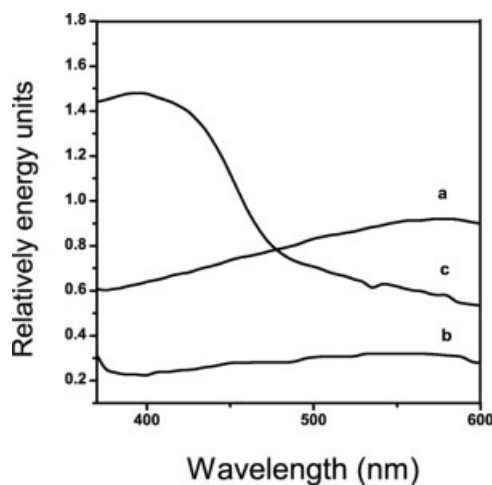
### Color change analyses

Figure 1 shows reflect spectrum of the samples. The graphs show that curves are different in the range of 370–600 nm visible lights. Figure 1(a,b) shows reflect curves of both PA6 and EPT are flatness. All light is absorbed in the region of visible wavelength. So, their colors are white. However, Figure 1(c) shows PA6EPT is green-yellow. There is absorption peak in 395 nm that belongs to purple light (380–450 nm), so its reflect light is green-yellow, complementarity of purple.<sup>1</sup>

### Analysis of hydrogen bonding

#### Hydrogen bonding status at room temperature

Figure 2 shows the FTIR spectra of PA6 and PA6EPT at room temperature in the ranges of 4000–2000 cm<sup>-1</sup>



**Figure 1** Visible light spectrogram of (a) pure PA6, (b) EPT, and (c) PA6EPT.

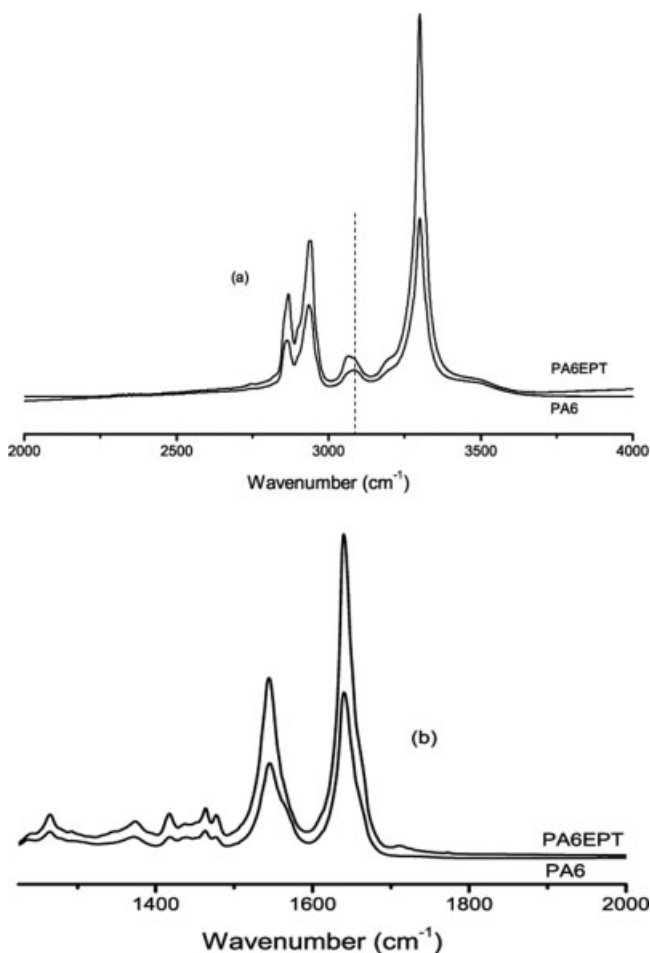


**Figure 2** Comparison of FTIR spectra at room temperature in the range of (a) 4000–2000  $\text{cm}^{-1}$  and (b) 2000–1225  $\text{cm}^{-1}$ .

and 2000–1225  $\text{cm}^{-1}$ . In the spectra, shift of many bands are tiny, except for the vibration shoulder absorbance position close by N–H band stretching absorption ranging from 3100 to 3000  $\text{cm}^{-1}$  in both spectroscopy. The shoulder peak related to hydrogen bonding of them, such as hydrogen bonded N–H stretching, amide I, amide II, and so forth are nearly the same. Therefore, compounding PA6 with EPT will considerably influence the status of hydrogen bonding at room temperature. The 3091  $\text{cm}^{-1}$  absorbance peak is generated in the interaction of amide I and amide II and affected by hydrogen bonding between N–H and C=O in PA6 chains. Figure 2 shows that the shoulder absorbance position shifts to low wavenumber, from 3091 to 3067  $\text{cm}^{-1}$ . The shift change is large. But other absorbance peaks have no shift phenomenon. Hydrogen bonding in PA6EPT is formed in condition of destroying the hydrogen bonding in PA6 chains, and come into being between N–H band in the PA6 molecular chains and C=O in EPT compound. And the sterically hindered effect was produced because of hydrogen bonding formed, both order of molecular

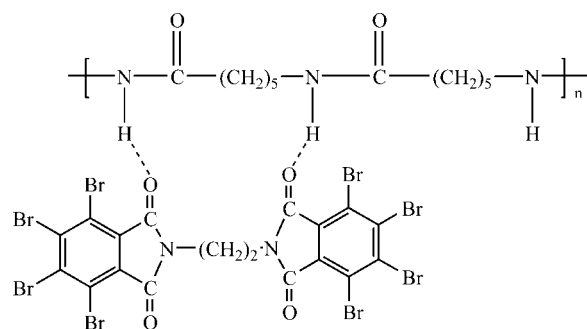


**Figure 3** A possible form of chromophore produced by hydrogen bonding between pure PA6 and EPT.

arrangement and motion of C–C bands are different by comparing with the molecular structure of PA6 and PA6EPT, and it has influenced the absorbance position. So, the shifts take place in IR spectra. It can be illustrated that hydrogen bonding have been formed between N–H group in PA6 and C=O polar functional group in EPT. There have 1710  $\text{cm}^{-1}$  absorbance peaks in the Figure 2(b). It is characteristic absorbance of C=O in EPT. And there are not new functional groups in the PA6EPT, which has been proved by  $^1\text{H-NMR}$  result. These facts illustrate that hydrogen bonding that is formed between PA6 and EPT is existent and effective in the process of producing color.

Figure 3 shows a possible form of a chromophore self-assembled by hydrogen bonding between PA6 and EPT. An intermolecular hydrogen bonding is formed between C=O group linking with phenyl and H atom in N–H group of molecule chain. The PA6 molecular chain and EPT molecule were connected by means of hydrogen bonding. And we can see that the structure is “bridge” shape, which is the same as the structure of tetrachloroisindolinones,<sup>1</sup> such as yellow pigment 109 and 110 (Fig. 4).

#### Hydrogen bonding change with temperature

Thermal stability of hydrogen bonding is related to the thermal mechanical properties of PA6 and aids

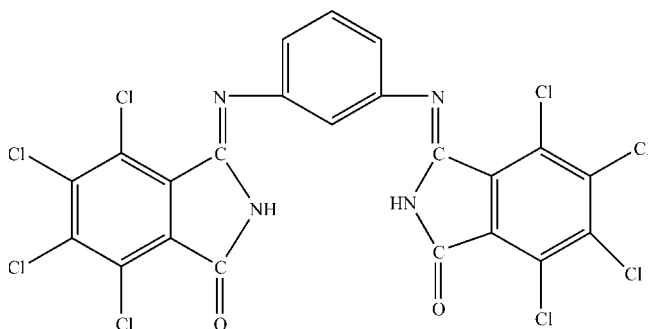


**Figure 4** The structure of pigment 109.

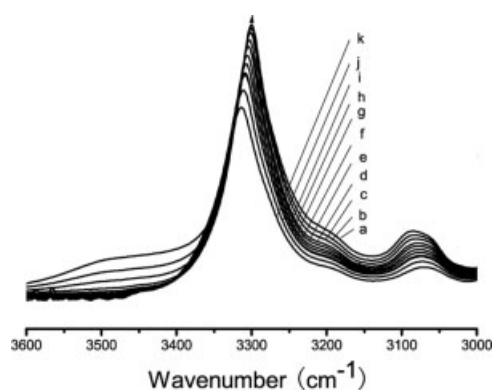


**Figure 5** High-resolution FTIR absorbance spectra of pure PA6, reported over 3600–3000  $\text{cm}^{-1}$  wavenumber ranges at 20°C intervals; significant peaks: 3300, 3085  $\text{cm}^{-1}$  at 30°C temperature. a: 30°C; b: 50°C; c: 70°C; d: 90°C; e: 110°C; f: 130°C; g: 150°C; h: 170°C; i: 190°C; j: 210°C; and k: 230°C.

to understanding the nature of hydrogen bonding. Temperature FTIR spectroscopy<sup>11–18</sup> is the usual methodology for investigating the status of hydrogen bonding at different temperatures. We will discuss the temperature FTIR spectrum of PA6 and PA6EPT, respectively. Since each spectrum contains many peaks over wavenumber range scanned (from 4000 to 450  $\text{cm}^{-1}$ ), the analysis to follow will focus on those typical peaks exhibiting greatest change with temperature.

Figures 5 and 6 show infrared spectra in the range of 3600–3000  $\text{cm}^{-1}$  of PA6 and PA6EPT recorded as a function of increasing temperature (30–230°C). As thermal energy is added, intramolecular and intermolecular forces will be overcome gradually. Thus, less energy is required to excite corresponding vibrational dipoles, and spectral peaks will appear at different wavenumbers as thermal energy drives mate-

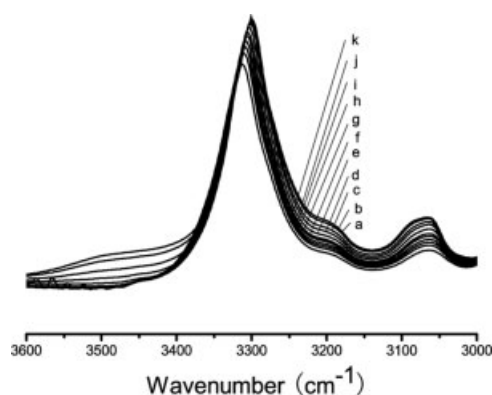


**Figure 6** High-resolution FTIR absorbance spectra of PA6EPT, reported over 3600–2800  $\text{cm}^{-1}$  wavenumber ranges at 20°C intervals; significant peaks: 3300, 3066  $\text{cm}^{-1}$  at 30°C temperature. a: 30°C; b: 50°C; c: 70°C; d: 90°C; e: 110°C; f: 130°C; g: 150°C; h: 170°C; i: 190°C; j: 210°C; and k: 230°C.

rials toward increasing disorder. In the Figures 5 and 6, 3400–3200  $\text{cm}^{-1}$  absorbance peaks decrease in intensity and shift to higher wavenumber position as temperature increases, and 3150–3000  $\text{cm}^{-1}$  peaks are dominated by a broad, nearly featureless plateau. The peak simply decreases in intensity coalescing into the broad plateau. This behavior is curious, especially considering hydrogen bonding.

Figure 7 presents the peak position of the PA6 and the PA6EPT taken as a function of the temperature. Figure 7(a) shows that the shift has taken place in the N–H stretching absorption position with increasing temperature in PA6 and PA6EPT. 3300  $\text{cm}^{-1}$  is the significant peak about –N–H stretching absorption. 3300  $\text{cm}^{-1}$  shifts to 3314  $\text{cm}^{-1}$  for PA6 and 3300  $\text{cm}^{-1}$  shifts to 3313  $\text{cm}^{-1}$  for PA6EPT. This peak behaves are very similar. The extent of disorder was enlarged with increasing temperature, because

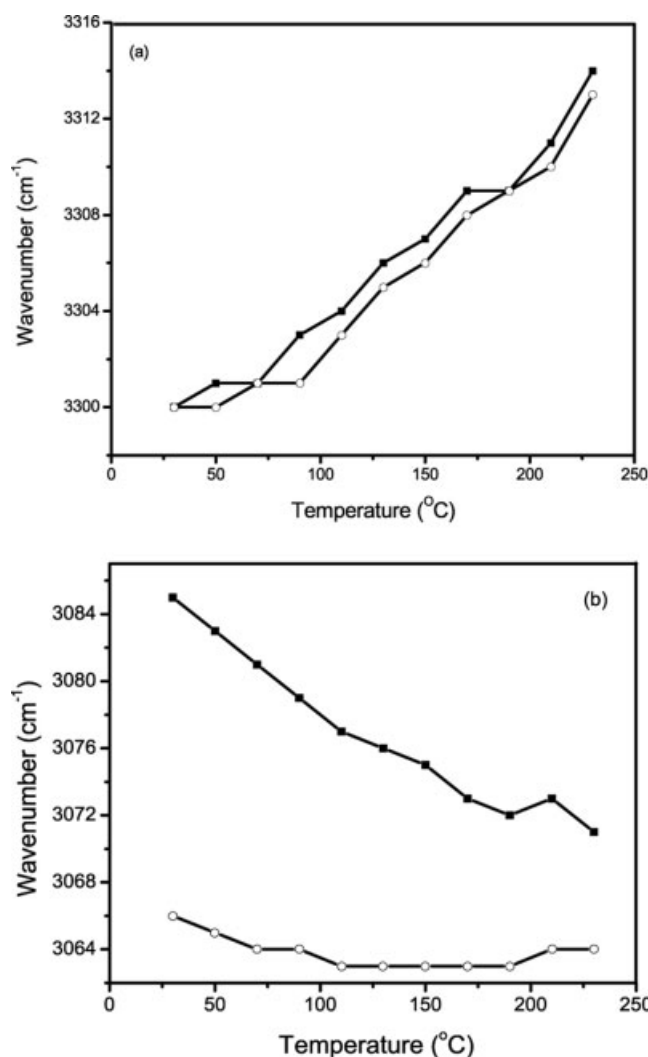


**Figure 7** Frequency shifts of (a) the –N–H band (3398–3316  $\text{cm}^{-1}$ ) and (b) the shoulder peak nearing the –N–H band (3086–3062  $\text{cm}^{-1}$ ) with increasing temperature in PA6 (■) and PA6EPT (○).

arrange of molecular chain was destroyed, that is to say, the portion of hydrogen bonding was destroyed with increasing temperature. And the surroundings around N—H band were changed. It leads to change of N—H band absorbance position.

Figure 7(b) shows that the absorption position at  $3085\text{ cm}^{-1}$  is shifting to  $3071\text{ cm}^{-1}$  with temperature increase in PA6,  $3066\text{ cm}^{-1}$  shifts to  $3064\text{ cm}^{-1}$  in the PA6EPT.  $3085\text{--}3062\text{ cm}^{-1}$  peaks are the position about N—H band vibrational shoulder absorption, which is brought by hydrogen bonding, which is formed between N—H group and other polar group. The direction of shift is contrary to  $3300\text{ cm}^{-1}$  absorption peak with increasing temperature. This peak shifts to lower wavenumber. Reason causing those shifts is related to stability of hydrogen bonding. Hydrogen bonding was destroyed with increasing temperature in the PA6 molecule. And bending vibration frequency is sensitive to temperature change because of the broken hydrogen bonding. It can be illustrated that the intramolecular hydrogen bonding in PA6 molecule chain is not stable due to the formation of three membered ring, which shows a sensitivity towards thermal energy. Therefore, the three membered ring sterically considered as highly energetic structure is easily broken with raising less amount of temperature. The tendency of broken hydrogen bonding will be enlarged with increasing temperature. But in the PA6EPT, the absorption position at  $3066\text{ cm}^{-1}$  is shifting to  $3064\text{ cm}^{-1}$  in the Figure 7(b). The peak position does not change much with temperature. And bending vibration frequency is low degree of sensitivity to temperature change, because hydrogen bonding, which was formed between PA6 and EPT in the high temperature, is not broke easily. And in the high temperature, hydrogen bonding has confined the motion of PA6 molecule chain, and the change of frequency distortion is small. In the Figure 7(b), comparing the shift number of shoulder peak, we can conclude that the stability of hydrogen bonding in the PA6EPT is higher than that in PA6.

The stability of hydrogen bonding can be investigated by the change of intensity, too. Figures 5, 6, and 8 show the change of N—H stretching of PA6 and PA6EPT with increasing temperature has a similar trend: the band shifting to high frequency, the intensity of band decreases, and the width of the band becomes broad, detecting attenuation and dissociation of hydrogen bonding. Nevertheless, the change rate for PA6EPT is considerably less. Although the decrease of intensity of hydrogen bonded N—H stretching does not reveal a direct change of the strength of hydrogen bonding because the absorption coefficient<sup>14,15</sup> is not constant with increasing temperature. The breadth of this band correlate directly with the degree of order in the samples—the

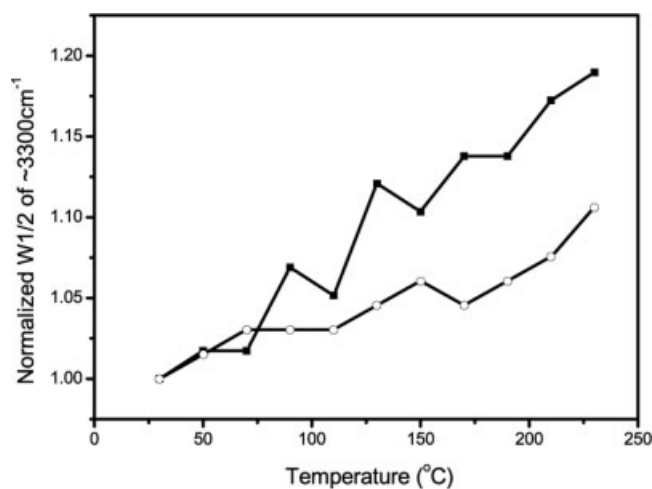


**Figure 8** Comparison of the temperature dependence of the width at half-height of the hydrogen-bonded N—H stretching band between PA6 (■) and PA6EPT (○).

broader the band is, the more disordered the samples.<sup>15</sup> Therefore, we compare the temperature dependence of bandwidth of the N—H stretching mode between PA6 and PA6EPT, as shown in Figure 8. The bandwidth was obtained by curve fitting to erase the influence of a two-phonon band at  $\sim 3200\text{ cm}^{-1}$  (the procedure is omitted). The bandwidths of N—H stretching in both PA6 and PA6EPT become larger steadily with increasing temperature, but the rate of increase of the bandwidth in PA6EPT is less than that in PA6. It means that the hydrogen bonding in PA6EPT is more stable than that in PA6.

#### Effect of hydrogen bonding on crystallization behavior

Figure 9 shows the IR spectra at range of  $3500\text{--}3000\text{ cm}^{-1}$  and  $1500\text{--}500\text{ cm}^{-1}$ . This is characteristic absorbance peaks of  $\alpha$ -phase and  $\gamma$ -phase. The peaks of  $\alpha$ -phase are  $3065, 1477\text{ cm}^{-1}$  ( $\text{CH}_2$  scissors vibration),<sup>19</sup>  $1416\text{ cm}^{-1}$  ( $\text{CH}_2$  scissors vibration),<sup>19</sup>  $1373\text{ cm}^{-1}$  (amide III and  $\text{CH}_2$  wag vibration),<sup>20</sup>  $1199\text{ cm}^{-1}$  ( $\text{CH}_2$  twist-wag vibration),<sup>21</sup>  $959\text{ cm}^{-1}$  ( $\text{CO—NH}$  in plane vibration),<sup>21</sup> and  $928\text{ cm}^{-1}$  ( $\text{CO—NH}$  in plane vibration).<sup>22</sup> The peaks of  $\gamma$ -phase are  $1439\text{ cm}^{-1}$  ( $\text{CH}_2$  scissors vibration),<sup>23</sup>  $1369\text{ cm}^{-1}$  ( $\text{CH}_2$  twist-wag vibration),<sup>19</sup>  $1236\text{ cm}^{-1}$  ( $\text{CH}_2$  twist-wag vibration),<sup>23</sup>  $976\text{ cm}^{-1}$  ( $\text{CO—NH}$  in plane vibration),<sup>24</sup>  $712\text{ cm}^{-1}$  (amide V).<sup>24,25</sup> Figure 9 shows strong features of the  $\alpha$ -phase associated with peaks at  $3065, 1477, 1416, 1373, 1199, 959,$  and  $928\text{ cm}^{-1}$ . In contrast, peaks of pure PA6 show that the  $\gamma$ -phase was dominant. According to the hypothetic formation of hydrogen bonding (Fig. 3), hydrogen bonding has restricted the twist-wag motion of PA6 chains. The arrangement of PA6 chains was propitious to form  $\alpha$ -phase.

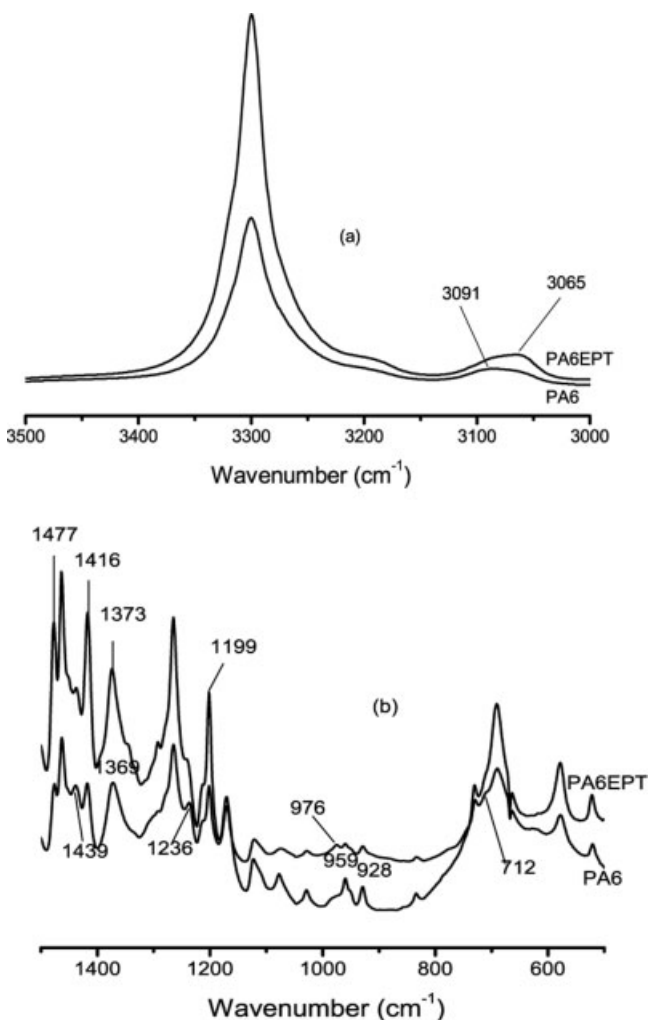


Figure 9 FTIR spectra of pure PA6 and PA6EPT in the range (a) 3500–3000  $\text{cm}^{-1}$  and (b) 1500–500  $\text{cm}^{-1}$ .

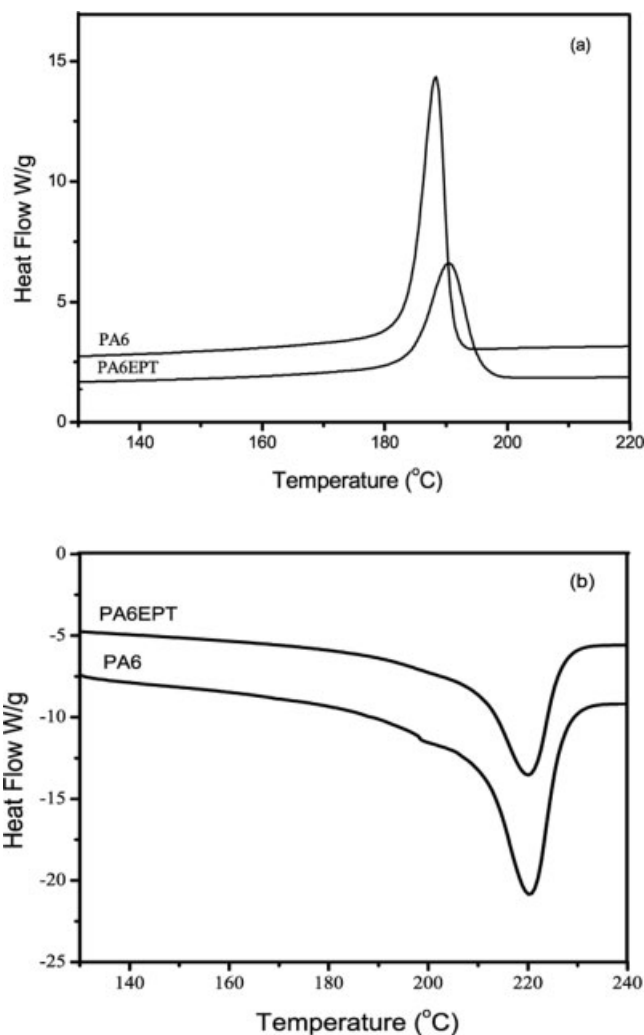


Figure 10 DSC (a) crystallization and (b) melting curves.

Differential scanning calorimetry analyses

The degree of crystallization is the most important characteristic of a polymer in that it determines mechanical properties, such as yield stress, elastic modulus, and impact resistance. So, DSC would be employed to analyze the effect of hydrogen bonding on the thermal behavior in this process. And we would simply compare the difference of data about DSC, such as crystallizing point, crystallizing enthalpy, melting point, and melting enthalpy. Figure 10 shows the crystallizing curve (a) and melting curve (b) of PA6 and PA6EPT, which were prepared under identical condition.

Table I summarizes data from Figure 10. In the Table I, the melting temperature ( $T_m$ ) of PA6EPT changed little with addition of EPT. But the peak temperature of crystallization ( $T_c$ ) of PA6EPT is higher than that of pure PA6. Since the compound EPT was added in the PA6, the hydrogen bonding of PA6EPT was formed in high temperature and

more stability than that of PA6. Hydrogen bonding in PA6EPT has improved the order of microchains in the course of decreasing temperature. It was favorable to the formation of crystal nucleus. So, crystallization temperature of PA6EPT increases, and the onset crystallization temperature and the increment rate of crystal nucleus in PA6EPT are larger than that in PA6. Although EPT can increase the rate of crystallization because of the nucleation effect,

TABLE I  
Values of  $T_c$ ,  $T_m$ ,  $\Delta T_c$ ,  $\Delta H_c$ ,  $\Delta H_m$  at 10°C/min Cooling Rate for Pure PA6 and PA6EPT

Samples	$T_c$ (°C)	$T_m$ (°C)	$\Delta T_c$ (°C)	$\Delta H_c$ (J/g)	$\Delta H_m$ (J/g)
Pure PA6	188.3	220.5	32.2	58.4	58.8
PA6 EPT	190.4	220.5	30.1	53.3	54.2

$T_c$ , the maximum crystallization rate temperature;  $T_m$ , melting temperature;  $\Delta T_c = T_m - T_c$ ;  $\Delta H_c$ , crystallization enthalpy;  $\Delta H_m$ , melting enthalpy.

pure PA6 is also easily to crystalline with a high crystallization rate, which causes no difference in melting point between PA6 and PA6EPT. But it is an accidental phenomenon. If the temperature rising rate increases, the sensitive degree of testing increases and the crystalline temperature is different. However, hydrogen bonding formed has restrained the action of chains and affected the ordering rate of chains and reduced the rate of crystal growing in the course of crystal growing. So the driving force ( $\Delta T_c$ ) of PA6EPT is lower than that of PA6. Despite PA6EPT has higher crystallizing temperature, its crystallizing enthalpy and melting enthalpy is lower (Table I), and then crystallinity of PA6EPT is lower than that of PA6. So it illustrated hydrogen bonding has effect of obstruct in the course of crystal growing.

### CONCLUSIONS

1. The change of color has been analyzed by visible chromatogram. Both PA6 and EPT are white; the color in blends of PA6 and EPT is green-yellow.
2. Existence of hydrogen bonding have been proved by FTIR; there is strong evidence of the intermolecular hydrogen bonding, which is of a unionized type between the PA6 molecular chain and the EPT, can self-assemble a chromophore.
3. The thermal stability of the intermolecular hydrogen bonding has been investigated by temperature-dependent FTIR. The results showed that the intermolecular hydrogen bonding in the PA6EPT is more stable than that in the PA6 molecular chain.
4. Hydrogen bonding formed between PA6 chains and EPT restricted motion of PA6 chains. Arrange of chains was fixed by hydrogen bonding. So it was of advantage to formation of  $\alpha$ -phase.
5. DSC has analyzed different of crystallization temperature and enthalpy. From above discussions, we know that the intermolecular hydro-

gen bonding in the PA6EPT is importance cause for the difference of crystallizing temperature.

### References

1. Gächter, R.; Müller, H. In *Plastics Additives Handbook*; Hanser Publishers: New York, 1983.
2. Lee, T. S.; Kim, D.-Y.; Jiang, X. L. *Macromol Chem Phys* 1997, 198, 2279.
3. Lee, T. S.; Kim, D.-Y.; Jiang, X. L.; Kumar, J. *J Polym Sci, Part A: Polym Chem* 1998, 36, 283.
4. Fiorini, C.; Prudhomme, N.; Etile, A. C.; Lefin, P.; Raimond, P. *Macromol Symp* 1999, 137, 105.
5. Lagugne-Labarthe, F.; Buffeteau, T.; Sourisseau, C. *Appl Phys B* 2002, 74, 12.
6. Yang, S.; Li, L.; Chilli, A. L.; Kumar, J.; Tripathy, S. K. *J Macromol Sci-Pure Appl Chem A* 2001, 38, 1345.
7. Liu, W.; Lee, S.-H.; Yang, S.; Bian, S.; Li, L.; Tripathy, S.K. *J Macromol Sci-Pure Appl Chem A* 2001, 38, 1355.
8. Sek, D.; Schab-Balcerzak, E.; Solyga, M.; Miniewicz, A. *Synth Metals* 2002, 127, 89.
9. Miniewicz, A.; Komorowska, K.; Sek, D.; Schab-Balcerzak, E.; Solyga, M. *Polish J Chem* 2002, 76, 395.
10. Zhiqiang, L. *J China Plastics Indus China* 2001, 29, 3.
11. Lillya, C. P.; Baker, R. J.; Hutte, S.; Winter, H. H. *Macromolecules* 1992, 25, 2076.
12. Trifand, D. S.; Terenzi, J. F. *J Polym Sci* 1958, 28, 443.
13. Schroeder, L. R.; Cooper, S. L. *J Appl Phys* 1976, 47, 4310.
14. Garcia, D.; Tarkweather, S. H. W. *J Polym Sci Polym Phys Ed* 1985, 23, 537.
15. Skrovanek, D. J.; Howe, S. E.; Painter, P. C.; Coleman, M. M. *Macromolecules* 1985, 18, 1676.
16. Skrovanek, D. J.; Painter, P. C.; Coleman, M. M. *Macromolecules* 2001, 19, 699.
17. Holland, B. J.; Hay, J. N. *Polymer* 2001, 42, 4759.
18. Macknight, W. J.; Yang, M. *J Polym Sci Polym Symp* 1973, 42, 817.
19. Schneider, B.; Schmidt, P.; Wichterle, O. *Coll Czech Commun* 1962, 27, 1749.
20. Doskocilova, D.; Pivcova, H.; Schnieder, B.; Cefelin, P. *Coll Czech Commun* 1963, 28, 1867.
21. Illers, K. H.; Haberkom, H.; Lanbo, J. B. *J Macromol Sci Phys B* 1972, 6, 129.
22. Rotter, G.; Ishida, H. *J Polym Sci, Part B: Polym Phys* 1992, 30, 489.
23. Tobin, M. C.; Carrano, M. J. *J Chem Phys* 1956, 25, 1044.
24. Arimoto, H. *J Polym Sci, Part A: Gen Pap* 1964, 2, 2283.
25. Miyake, A. *J Polym Sci* 1960, 44, 223.